*Article*

Frost Resistance and Shrinkage Characteristics of Soil Stabilized by Carbide Slag and Coal Gangue Powder

Quanman Zhao [1,*], **Jianshu Liu** [1], **Li Wu** [1], **Xiaojin Lu** [1], **Hao Li** [1], **Wenjun Hu** [1,*], **Yongsheng Zhang** [2], **Xianghui Kong** [1] **and Shuo Jing** [1]

1   School of Traffic Engineering, Shandong Jianzhu University, Jinan 250101, China
2   Shandong Road & Bridge Construction Group Co., Ltd., Jinan 250102, China
*   Correspondence: zhaoquanman@sdjzu.edu.cn (Q.Z.); huwenjun@sdjzu.edu.cn (W.H.)

Abstract: With the increase of expressway construction in seasonal frozen soil region, the freeze-thaw problem of subgrade soil has attracted more and more attention. In addition, the comprehensive utilization of industrial solid waste has become an important measure to build a resource-saving and environment-friendly society. In order to improve the frost resistance of subgrade soil and realize the resource utilization of industrial solid waste, carbide slag (CS) and coal gangue powder (CG) were applied to the subgrade soil. The unconfined compressive strength (UCS) test, freeze-thaw cycle test, dry shrinkage test, temperature shrinkage test and scanning electron microscope (SEM) test were carried out on CS-CG stabilized soil with a ratio of CS:CG = 70:30 and dosages of 5%, 10% and 15%. The freeze-thaw cycle degradation model of CS-CG stabilized soil was constructed to show the freeze-thaw deterioration mechanism after the mechanical properties, pore structure, and durability characteristics of the stabilized soil were examined. The results showed that the CS-CG stabilized soil had good frost resistance. After 6 freeze-thaw cycles, the UCS at 7d and 28 d was 2.86 MPa and 3.79 MPa, respectively, which were 22.6% and 35.5% lower than in samples that underwent no freeze-thaw action. The CS-CG stabilized soil had good crack resistance, slightly better dry shrinkage strain than lime stabilized soil, and excellent temperature shrinkage performance. With the increase of CS-CG dosage, the hydration products increased continuously. After freeze-thaw cycles, however, large pores and cracks gradually appeared in the stabilized soil, which led to an increase of porosity and pore diameter, and a decrease of pore abundance. Due to the influence of hydration degree, the porosity change at 7 d was less than that at 28 d. There was a $f(n)/f_0 = \beta \exp(-\lambda \Delta h)$ relationship between UCS residual ratio and porosity variation of the CS-CG stabilized soil, and it had a good correlation. The CS-CG stabilized soil had good frost resistance and shrinkage characteristics, and could replace traditional cementitious materials such as Portland cement (PC) and lime for subgrade soil improvement in regions with seasonal frozen soil. Future research needs to focus on the performance regulation of CS-CG stabilized soil, which can make it more widely used.

Keywords: road engineering; carbide slag; coal gangue; stabilized soil; frost resistance; shrinkage characteristics; deterioration model

1. Introduction

China is a vast country with a large north-south span and large climatic differences, among which seasonal frozen soil reaches 53.5% [1]. With the development of the western region and the proposal of the "Belt and Road" initiative, a large number of infrastructures have been built in regions with seasonal frozen soil, and more than 2/3 of roads in China cross regions with seasonal frozen soil [2,3]. Seasonal frozen soil will experience periodic freeze-thaw action with the change of external temperature, which causes frost heave and other damage to subgrade soil, and poses a great threat to road safety and stability [4].

To solve the problem of freeze-thaw disease in seasonal frozen soil, most scholars use traditional cementitious materials such as Portland cement (PC) [5] and lime [6] to

increase the frost resistance of subgrade soil. It has been found that the above two materials can reduce the strength reduction caused by freeze-thaw cycle and the expansion and contraction characteristics to varying degrees [7]. However, considering the pursuit of carbon emissions reduction, pressure concerning environmental protection in various regions has increased. The production of traditional cementitious materials such as lime and PC is limited and the price is soaring. Therefore, for the sake of environmental protection and sustainable development, some researchers have begun to apply industrial wastes such as carbide slag (CS), fly ash (FA), silica fume (SF) and coal gangue (CG) to the manufacture of cementitious materials [8–10]. Chen et al. used FA as the cementitious material to improve cohesive soil and carried out a series of frost resistance tests. It was found that 28 d FA based geopolymer reinforced soil can resist more than 1 freeze-thaw cycle, up to 6 cycles [11].

CS is a by-product of the reaction between water and carbide to produce acetylene gas and its main component is $Ca(OH)_2$. Therefore, CS can react with active compositions such as activated silica and activated alumina to produce the cementing material [12,13]. Recently, CS has been widely used as an alkali activator in the preparation of various geopolymers. It has been discovered that the addition of CS can somewhat increase the strength and durability of geopolymers [14–16]. CS is also directly used to replace PC to improve soil properties. Research has shown that with aging, the compressive strength of CS stabilized soil increases significantly [17,18]. Li et al. have established a forecasting model for unconfined compressive strength (UCS) of CS stabilized soil. The results revealed that the UCS increased linearly as compaction degree grew, logarithmically as curing age increased, and considerably as CS dosage increased [19]. Coal gangue (CG) is one of the main by-products produced during coal mining and production, accounting for 10–25% of total coal mining output, and its main component is silica-alumina oxide [20,21]. Over the years, the production of CG has increased day by day, occupying large tracts of land and causing serious environmental pollution [22]. Therefore, some scholars have used it as concrete aggregate instead of natural aggregate, and found that CG aggregate has the problems of high water absorption rates and porosity. The higher the degree of replacement of natural aggregate, the lower the compressive strength of concrete [20,23]. Some scholars have also directly applied CG powder to the improvement of expansive soil. According to studies, expansive soil expansion and contraction rates were reduced, and its shear strength was raised. [24]. However, the related research on the freeze-thaw characteristics of the coal gangue powder and carbide slag composite improved subgrade soil is basically blank. In addition, CS and CG are inexpensive and abundant, and it is feasible to use them replace PC or lime for subgrade soil improvement.

In this study, it mainly discussed the freeze-thaw characteristics and shrinkage characteristics of subgrade soil improved by coal gangue and carbide slag. In addition, the feasibility of its application in seasonal frozen soil region was explored. To test its UCS, frost resistance and shrinkage characteristics, the UCS test, freeze-thaw cycle test, dry shrinkage test, temperature shrinkage test and scanning electron microscope (SEM) test were carried out on CS-CG stabilized soil with the ratio of CS:CG = 70:30 and dosages of 5%, 10% and 15%. The strength development and freeze-thaw degradation mechanism of the CS-CG stabilized soil were revealed by observing the pore properties and distribution with Image-Pro Plus (IPP) software. [25–27]. Finally, the freeze-thaw degradation model of the CS-CG stabilized soil based on porosity change was established. As a comparison, the UCS, frost resistance and shrinkage characteristics of 4% PC stabilized soil and 12% lime stabilized soil were tested. The advantages and disadvantages of the CS-CG stabilized soil were analyzed. This study makes up for the research gap of freeze-thaw characteristics and shrinkage characteristics of CS-CG stabilized soil, and provides a reference for solving the freeze-thaw problem of seasonal frozen soil.

2. Materials and Methods

2.1. Materials

(1) Subgrade Soil

The soil was sourced from a section of the Mingdong Expressway project in Shandong Province, China. Table 1 and Figure 1 display its fundamental mechanical and physical characteristics as well as its gradation. According to the 'Test methods of soils for highway engineering' JTG 3430-2020 [28], the soil is a low liquid limit silty clay.

Table 1. Basic physical and mechanical properties of the subgrade soil.

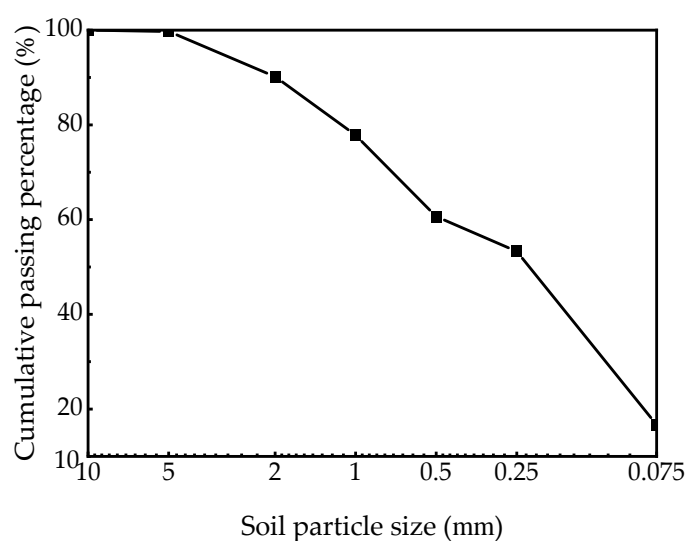| Material	Maximum Dry Density (g/cm^3)	Optimum Moisture Content (%)	Liquid Limit (%)	Plastic Limit (%)	CBR (%)	Modulus of Resilience (MPa)
Soil	2.018	8.5	29.4	16.2	5.6	51.5

Figure 1. Gradation of the subgrade soil.

(2) CS, CG, PC and lime

The CS was produced by Anyang Xinhai Metallurgy Co., Ltd., Henan Province, China, with a fineness of 200 mesh. The CG was produced by Hebei Jinghang Mineral Products Co., Ltd., Shijiazhuang City, China, with a fineness of 325 mesh, and to increase its activity, it was calcined at 900 °C [29] to obtain the CG powder used. The P.O425 PC was acquired from Weifang Yangchun Co., Ltd., Anqiu City, China. The lime was produced by Huihui Industrial Co., Ltd., Xinyu City, China. The chemical constitution of each substance was determined by X-ray fluorescence (XRF) test using ARL Advant X Intellipower 3600 equipment. Table 2 provided evidence of this, which showed that the main component of CS was CaO, accounting for 92.24%. The main components of CG were SiO_2 and Al_2O_3, accounting for 48.33% and 48.95%, respectively. The PC primarily consisted of SiO_2 and CaO, accounting for 20.35% and 61.11%, respectively. The lime was composed mainly of CaO, accounting for 93.11%.

Table 2. Chemical compositions of CS, CG, PC, and Lime.

Material	SiO$_2$	Al$_2$O$_3$	CaO	Fe$_2$O$_3$	TiO$_2$	K$_2$O	MgO	SO$_3$	Na$_2$O	ZnO	MnO	P$_2$O$_5$	Cl$^-$	Other
CS	3.64	2.04	92.24	0.62	0.10	0.04	0.15	1.04	0.02	—	—	0.02	0.05	0.05
CG	48.33	48.95	0.21	0.66	1.26	0.15	0.14	0.04	0.06	0.01	—	0.02	0.05	0.05
PC	20.35	4.60	61.11	4.88	0.87	0.40	3.13	2.34	0.29	—	0.26	—	—	1.77
Lime	1.87	0.51	93.11	0.12	—	—	2.85	0.55	0.01	—	—	0.13	0.01	0.84

(3) Alkali activator

In the preparation of the CS-CG stabilized soil, to improve the activity of oxides in CS and CG, an NaOH and Na_2SiO_3 mixed solution was used as the alkali activator. The NaOH was produced by Shandong Binhua Dongrui Chemical Co., Ltd., Binzhou, China and the Na_2SiO_3 was produced by Tianjin Bohai Dongfanghong Chemical Co., Ltd., Tianjin, China.

(4) Water

The water was from Jinan city municipal water.

2.2. Methods

(1) Specimen preparation

After a preliminary exploratory test, the ratio of CS:CG = 70:30 was found to be reasonable. The CS-CG dosages were 5%, 10% and 15%. Three dosages of CS-CG stabilized soil, 4% PC stabilized soil and 12% lime stabilized soil with curing ages of 7 d and 28 d were prepared. During the preparation of the CS-CG stabilized soil, the alkali activator NaOH and Na_2SiO_3 were mixed at a quality ratio of 1:1 and evaporated in pure water. The concentration of NaOH was 8 mol/L, and the quality ratio of alkali-activated solution to CS-CG was 0.5. Referring to 'Test Methods of Materials Stabilized with Inorganic Binders for Highway Engineering' JTG E51-2009 [30], cylindrical specimens with a size of 50 mm × 50 mm and trabecular specimens with a size of 50 mm × 50 mm × 200 mm were prepared. The degree of compaction was 98%. Immediately after specimens were prepared, they were put in a standard curing box and kept there until they reached the appropriate age at a temperature of 21 ± 2 °C and a relative humidity of 95%.

(2) UCS test

UCS tests of three dosages of the CS-CG stabilized soil, 4% PC stabilized soil and 12% lime stabilized soil at different ages were carried out. 5 groups of specimens were prepared, with 6 in each group. The UCS was analyzed, and the optimum dosage of CS-CG stabilized soil was determined. The automatic compressive and flexural testing machine (YAW-300E) produced by Jinan Kaide Instrument Co., Ltd. was the instrument utilized in this test.

(3) Freeze-thaw cycle test

Referring to 'Test Methods of Materials Stabilized with Inorganic Binders for Highway Engineering' JTG E51-2009, CS-CG stabilized soil under the best dosage, 4% PC stabilized soil and 12% lime stabilized soil underwent freeze-thaw cycle tests. The test adopted the method of freezing for 16 h and thawing for 8 h. Freeze-thaw cycle tests were carried out in a high-low temperature test chamber with a minimum freezing temperature of −18 °C. 0~6 freeze-thaw cycles were performed on the different stabilized soils. Each freeze-thaw cycle consisted of 6 specimens, and a total of 126 specimens (3 kinds of stabilized soil × 6 specimens × 7 cycles) were prepared. After the freeze-thaw cycles, the UCS and quality change rate (QCR) of each specimen were tested to analyze the frost resistance.

(4) Shrinkage test

To determine the shrinkage characteristics of the CS-CG stabilized soil, the dry shrinkage and temperature shrinkage test on the CS-CG stabilized soil under the best dosage, 4% PC stabilized soil and 12% lime stabilized soil were carried out by referring to 'Test Methods of Materials Stabilized with Inorganic Binders for Highway Engineering' JTG E51-2009. Six specimens, three for measuring shrinkage strain and the other three for measuring water loss rate, were prepared from each group for the dry shrinkage test. Three specimens from each group of the temperature shrinkage test were made. Therefore, a total of 27 trabecular specimens (3 stabilized soils × 6 dry shrinkage specimens + 3 stabilized soils × 3 temperature shrinkage specimens) were prepared.

(5) SEM test

On the CS-CG stabilized soil, SEM tests were carried out using various dosages and the optimal dosage during various freeze-thaw cycles. The microscopic characteristics were analyzed to reveal the strength formation and freeze-thaw cycle degradation mechanism. The equipment used was HITACHI Schottky Field Emission Scanning Electron Microscope SU5000 with a magnification of 8000 times. To analyze the distribution of porosity, pore

diameter and pore abundance of the optimum dosage CS-CG stabilized soil from 0 to 6 freeze-thaw cycles at 7 d and 28 d, MATLAB software and IPP software was employed in the SEM images processing. Frost resistance was examined under a microscope to disclose the deterioration mechanism under freeze-thaw cycles and to explore the impact of these cycles on pores. The calculation formula for porosity, which is defined as the proportion of the total pore area, is provided in Equation (1):

$$P = \frac{\sum_{i=1}^{N} S_i}{S_{total}} \times 100 \tag{1}$$

where S_i is the area of the *i*-th pore (μm^2), N is the total number of pores, Stotal is total image area (μm^2).

The pore diameter is the average diameter (μm) through the pore centroid. The ratio of a pore's short axis to the long axis is known as Pore abundance, as shown in Equation (2):

$$C = \frac{B}{L} \tag{2}$$

where B is the short axis of the pore, L is the long axis of the pore.

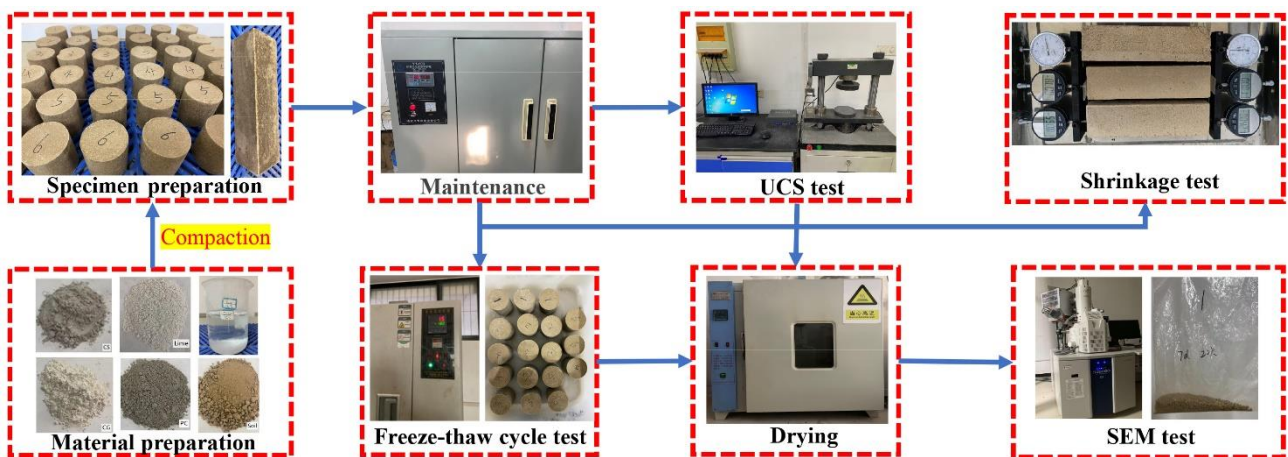In Figures 2 and 3, the test procedure and equipment and test flow chart are depicted.

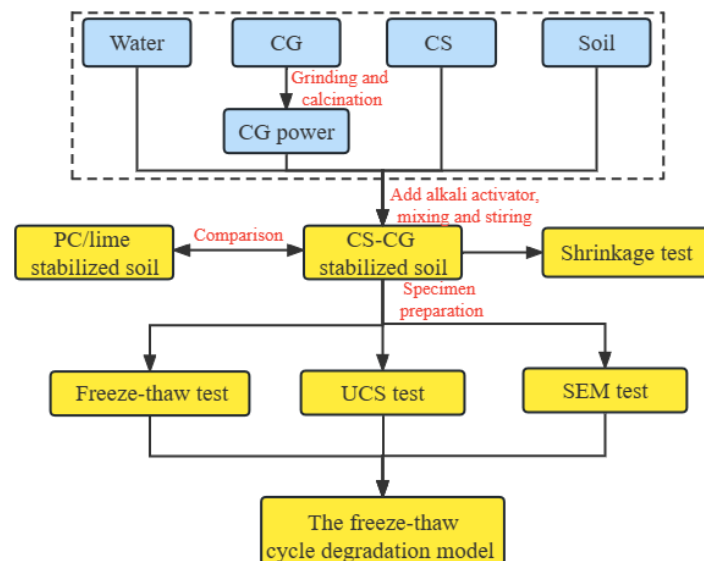**Figure 2.** The test process and equipment.

Figure 3. The test flow chart 3. Test results and analysis.

3. UCS Test Results and Analysis

The results of UCS tests at different ages are shown in Figure 4. As depicted in Figure 4, it can be seen that:

a.   The UCS of the 5%, 10% and 15% CS-CG stabilized soil at 7 d was 2.66 MPa, 3.68 MPa and 4.59 MPa, respectively. The UCS of 15% CS-CG stabilized soil was 12.6% larger than PC stabilized soil, and that of the 10% CS-CG stabilized soil was 8.2% smaller than, but they were much larger than lime stabilized soil.

b.   The UCS of the 5%, 10% and 15% CS-CG stabilized soil at 28 d was 4.81 MPa, 5.88 MPa and 6.87 MPa, respectively. They increased to varying degrees, with the 10% CS-CG stabilized increasing the most. At this time, the UCS of PC stabilized soil was 6.14 MPa, and the 10% CS-CG stabilized soil was close to it.

c.   Comparing the UCS of the three dosages of CS-CG stabilized soil with the two other kinds of stabilized soil at different ages, it can be seen that the UCS of 10% CS-CG stabilized soil was higher. Compared with the other two dosages of CS-CG stabilized soil, the UCS of the 10% CS-CG stabilized soil grew continuously, and the UCS at 28 d was close to 4% PC stabilized soil, so can be used as a subgrade filler to replace PC stabilized soil.
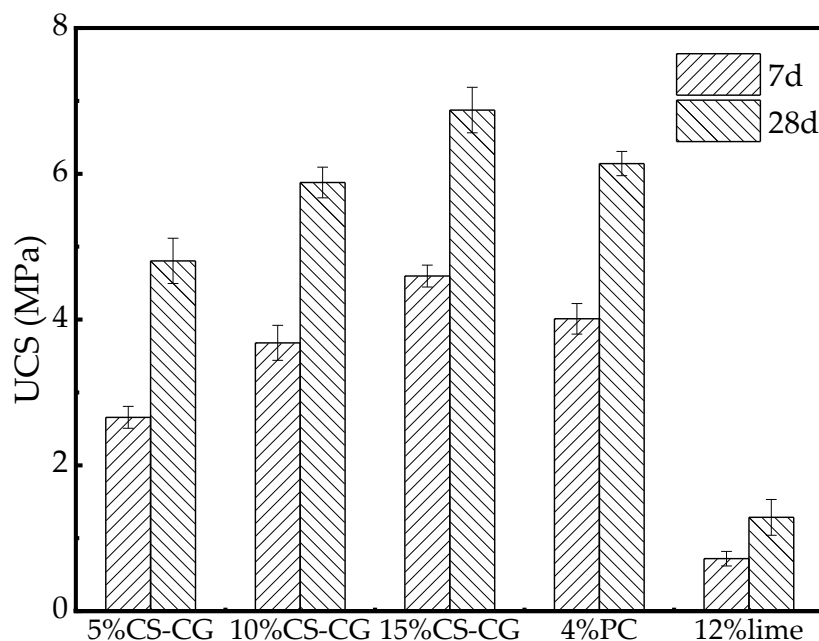

Figure 4. Results of UCS tests at different ages.

In summary, the UCS of CS-CG stabilized soil is higher than that of lime stabilized soil, which is close to that of PC stabilized soil. Compared with previous studies, the performance of CS-CG stabilized soil is better than that of fly ash-based polymer stabilized soil and carbide slag stabilized soil [10,18], which can be used as a subgrade filler to replace cement stabilized soil (Figure 4).

3.1. Freeze-Thaw Cycle Test Results and Analysis

Freeze-thaw cycle tests of CS-CG stabilized soil at 7 d and 28 d were carried out to analyze its frost resistance.

(1) Freeze-thaw cycle test results and analysis at 7 d

Due to the obvious frost heave after 1 freeze-thaw cycle, the lime stabilized soil was broken. Therefore, only the freeze-thaw cycle test results of the 4% PC stabilized soil and the 10% CS-CG stabilized soil at 7 d were compared. The test results of 7 d freeze-thaw cycles are shown in Figure 5.
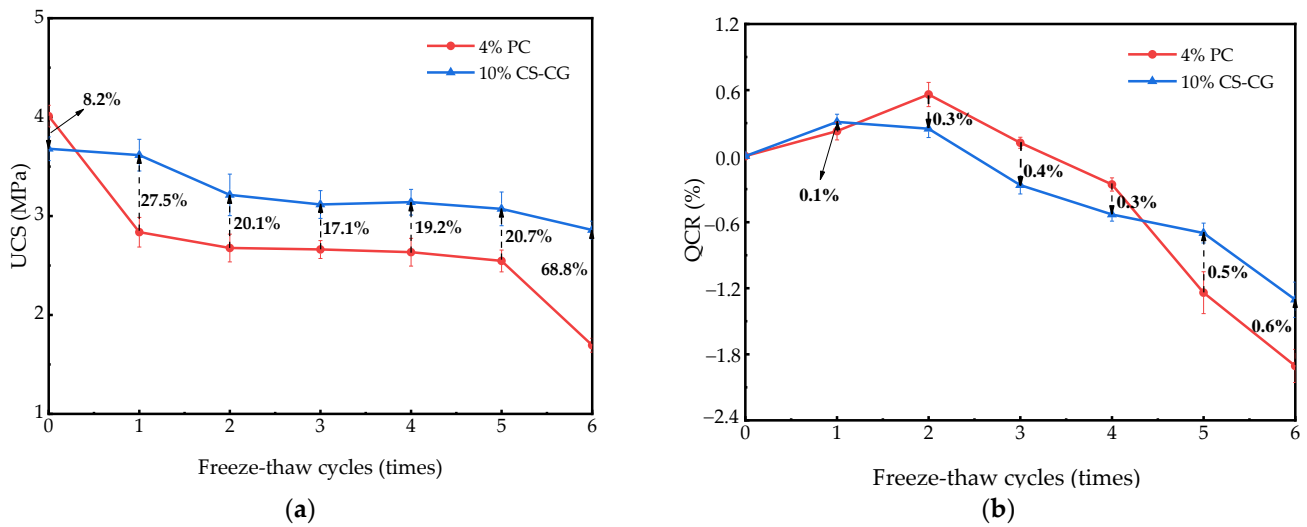
(**a**)

(**b**)

Figure 5. Test results of 7 d freeze-thaw cycles. (**a**) UCS test results and (**b**) QCR test results.

Figure 5 demonstrated that,

a. After the freeze-thaw cycles, the UCS of PC stabilized soil decreased sharply, decreasing by 29.2% after 1 freeze-thaw cycle, and the UCS of CS-CG stabilized soil decreased by 1.9%. At this time, the UCS of CS-CG stabilized soil was 27.5% larger than PC stabilized soil.

b. As the freeze-thaw cycles increased, the UCS of CS-CG stabilized soil decreased slightly, and the strength loss rate (SLR) was 22.6% after 6 freeze-thaw cycles. Meanwhile, the UCS of the CS-CG stabilized soil was 1.7 MPa, and the SLR reached 62.5%. The frost resistance of CS-CG stabilized soil was better than PC stabilized soil.

c. The QCR of both stabilized soils demonstrated a tendency of increasing and subsequently decreasing during freeze-thaw cycles, which was related to the freeze-thaw damage of the specimens in the later stage of water absorption. After 6 freeze-thaw cycles, the quality of PC stabilized soil decreased by 1.9%, and CS-CG stabilized soil decreased by 1.3%. It was evident that the effect of CS-CG stabilized soil was better than PC stabilized soil.

(2) Freeze-thaw cycle test results and analysis at 28 d

The test results of 28 d freeze-thaw cycles of the three stabilized soils are displayed in Figure 6.
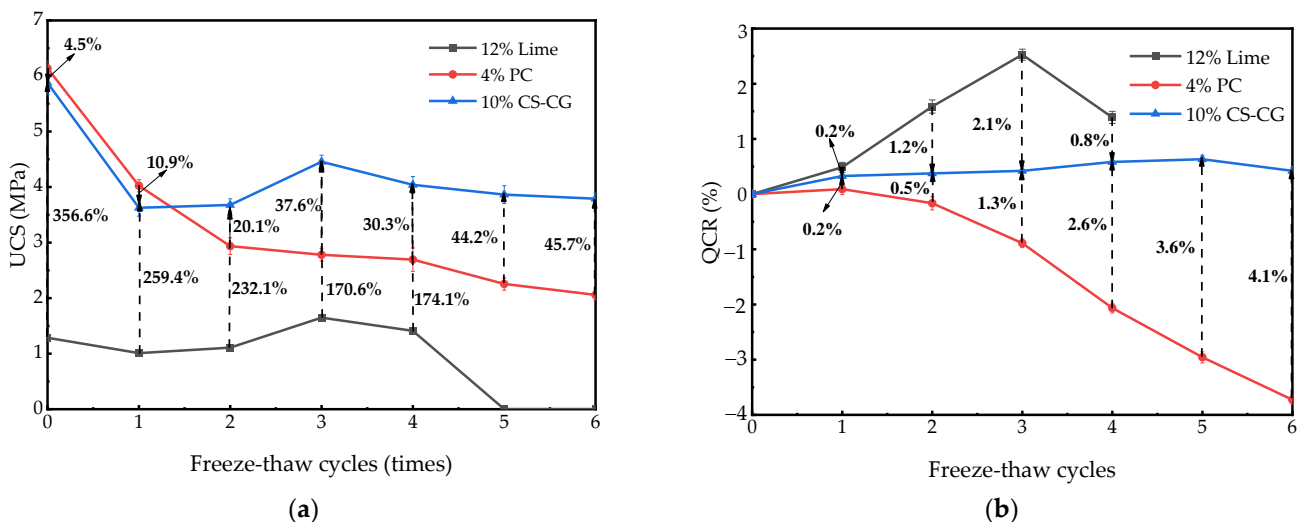

(**a**)

(**b**)

Figure 6. Test results of 28 d freeze-thaw cycles. (**a**) UCS test results and (**b**) QCR test results.

Figure 6 demonstrated that,

a. With an increase in freeze-thaw cycles, the UCS of CS-CG stabilized soil showed a tendency of decreasing sharply first, then increasing and subsequently decreasing, while the PC stabilized soil decreased continuously. The lime stabilized soil was below 2 MPa, and the frost heave failure of specimens occurred after 4 freeze-thaw cycles, meaning follow-up tests could not be carried out.

b. After 6 freeze-thaw cycles, the residual strength of the CS-CG stabilized soil was 3.79 MPa. Its SLR was 35.5%, which was obviously better than the 66.4% of the PC stabilized soil, showing that the CS-CG stabilized soil had good frost resistance at 28 d.

c. The QCR of the three stabilized soils showed three different trends. The quality of lime stabilized soil increased the most, and the tendency increased first and subsequently decreased. The PC stabilized soil decreased continuously, and the quality loss was 3.7% after 6 freeze-thaw cycles. The QCR of CS-CG stabilized soil was less than 1.0%, and there was basically no change. The frost resistance of the CS-CG stabilized soil at 28 d was better than lime stabilized soil and PC stabilized soil.

In summary, CS-CG stabilized soil has great advantages over PC stabilized soil and lime stabilized soil in strength loss rate and mass loss rate, and has good freeze-thaw characteristics, which is suitable for subgrade filling in seasonal frozen soil region. However, with the difference of soil, fineness of cementitious materials and alkali activator, there may still be differences. Therefore, further research on the freeze-thaw characteristics of different factors is needed in the future.

3.2. Shrinkage Test Results and Analysis

3.2.1. Dry Shrinkage Characteristics
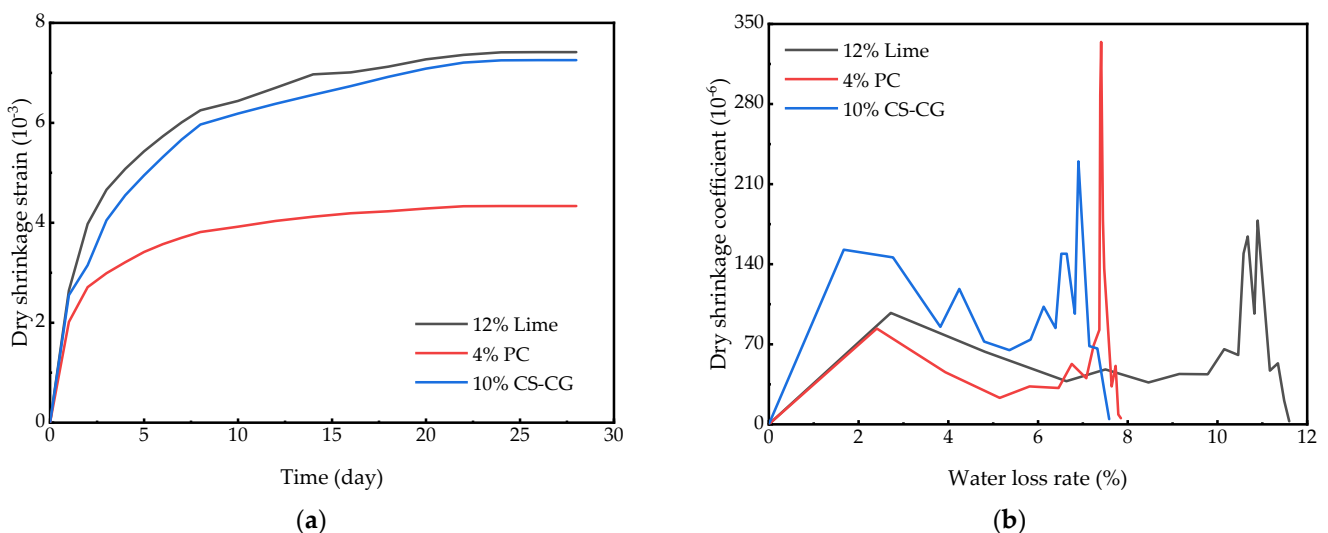
Figure 7 displays the test results of the dry shrinkage.

Figure 7. Dry shrinkage test results. (**a**) Variation of cumulative dry shrinkage strain with time and (**b**) Variation of dry shrinkage coefficient with water loss rate.

Figure 7 demonstrated that,

a. As time goes on, the dry shrinkage strain of three stabilized soils increased continuously, with rapid growth from 0 to 10 days, and then stabilized. The dry shrinkage strain of the 12% lime stabilized soil, the 4% PC stabilized soil and the 10% CS-CG stabilized soil was 4.3×10^{-3}, 7.2×10^{-3} and 7.3×10^{-3}, respectively. The PC stabilized soil had the best anti-dry shrinkage effect, and the CS-CG stabilized soil was slightly better than lime stabilized soil.

b.   The water loss rate of lime stabilized soil was the largest, reaching 11.6%. The rate of CS-CG stabilized soil was slightly smaller than PC stabilized soil, both of which were below 8%. Water loss rate directly determines the crack resistance [31], and the CS-CG stabilized soil had good crack resistance.

c.   The dry shrinkage coefficient of PC stabilized soil was up to 334.3×10^{-6}, but its total dry shrinkage coefficient was the smallest. The total dry shrinkage coefficient of the lime stabilized soil was the largest, and its peak value was the smallest, and the CS-CG stabilized soil was between the two.

The dry shrinkage characteristics of CS-CG stabilized soil fell between the PC stabilized soil and lime stabilized soil, and had good crack resistance.

3.2.2. Temperature Shrinkage Characteristics

Figure 8 displays the temperature shrinkage coefficients (TSC) in different temperature ranges.
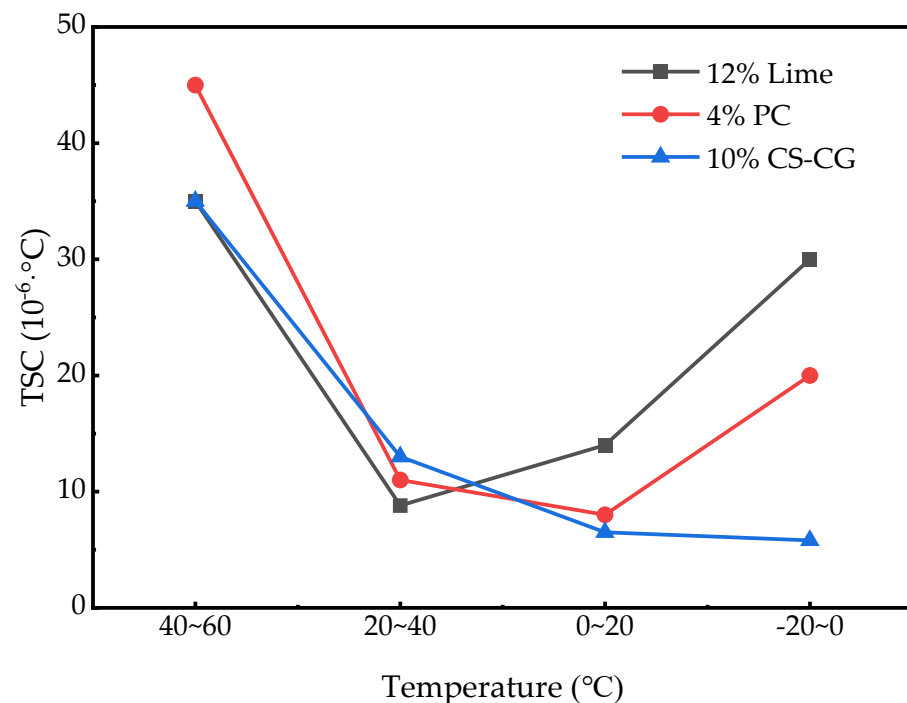

Figure 8. TSC in different temperature ranges.

Figure 8 demonstrated that,

a.   The CS-CG stabilized soil had good low temperature resistance. Its TSC was 5.8×10^{-6} in the range of $-20\text{~}0$ °C, which was far less than lime stabilized soil and PC stabilized soil.

b.   Compared with the lime stabilized soil, the CS-CG stabilized soil had good high temperature resistance. In the range of $40\text{~}60$ °C, its TSC was consistent with PC stabilized soil, both of which were 3.5×10^{-5}.

c.   In the two ranges of $0\text{~}20$ °C and $20\text{~}40$ °C, the TSC of the three stabilized soils were not much different, at less than 1.5 thr^{-5}, indicating that the CS-CG stabilized soil has a wide range of applications.

The TSC of the CS-CG stabilized soil was better than lime stabilized soil and PC stabilized soil. The low temperature resistance was outstanding, and the frost heave phenomenon, similar to the lime stabilized soil, did not easily occur.

3.3. SEM Test Results and Analysis

3.3.1. SEM Test Results and Analysis of Different Dosages of CS-CG Stabilized Soil

The SEM test results of the different CS-CG stabilized soils with different dosages are displayed in Figure 9. It demonstrated that the primary hydration products of CS-CG stabilized soil were C-(A)-S-H gel and $Ca(OH)_2$ crystal. With an increase in CS-CG dosage, the hydration products increased continuously, and the soil was continuously wrapped. Furthermore, the pores and cracks were obviously improved, which was why the UCS increased as the dosage is increased.
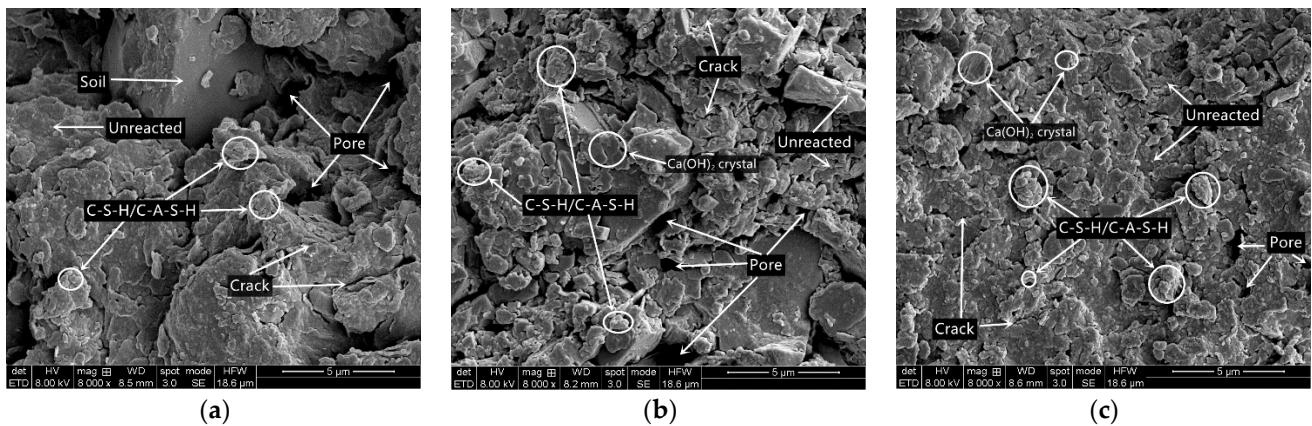

(a)　　　　　　　　　　(b)　　　　　　　　　　(c)

Figure 9. SEM test results of the CS-CG stabilized soils with different dosages. (**a**) 5%, (**b**) 10% and (**c**) 15%.

3.3.2. SEM Test Results and Analysis of the CS-CG Stabilized Soil under Different Freeze-Thaw Cycles

The SEM test on CS-CG stabilized soil under different freeze-thaw cycles at 7 d and 28 d was carried out to analyze its performance decay mechanism.

(1) 7 d

The SEM test results of the CS-CG stabilized soil with different freeze-thaw cycles at 7 d are displayed in Figure 10. It demonstrated that with an increase in freeze-thaw cycles, cracks and large pores appeared in the stable soil, especially after 6 cycles the pores increased and enlarged. However, at the same time, the hydration products also increased with freeze-thaw cycles. In the later stage of freeze-thaw cycles, monosulfoaluminate hydrate (AFm) appeared, which was related to the circulation process to promote the further hydration.
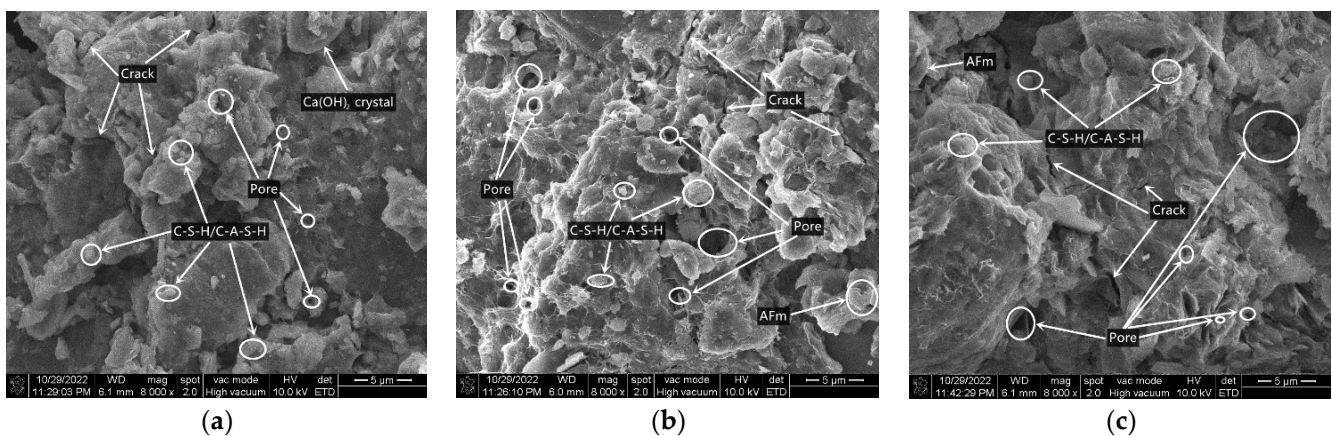

(a)　　　　　　　　　　(b)　　　　　　　　　　(c)

Figure 10. SEM test results of the CS-CG stabilized soil with different freeze-thaw cycles at 7 d. (**a**) 2 cycles, (**b**) 4 cycles and (**c**) 6 cycles.

(2) 28 d

The SEM test results of the 28d CS-CG stabilized soil under different freeze-thaw cycles are displayed in Figure 11. It demonstrated that the amount of hydration products of the stabilized soil at 28 d was much larger than that at 7 d, and the cracks and pores were less after 4 freeze-thaw cycles. It displayed that the freeze-thaw cycles had little effect at this time. After 6 freeze-thaw cycles, as with at 7 d, there was a more obvious pore structure.
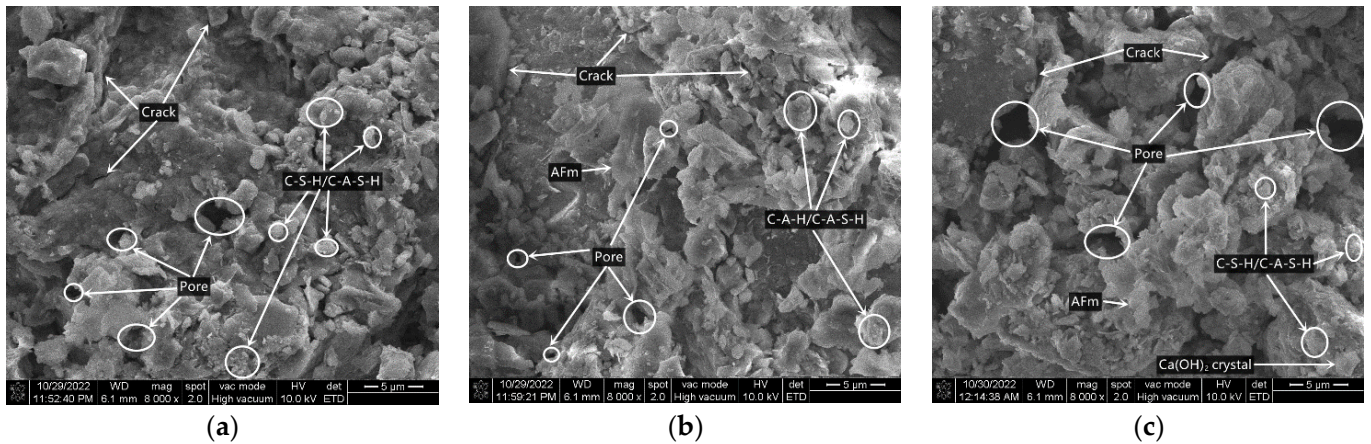

(**a**)　　　　　　　　　　(**b**)　　　　　　　　　　(**c**)

Figure 11. SEM test results of the CS-CG stabilized soil with different freeze-thaw cycles at 28 d. (**a**) 2 cycles, (**b**) 4 cycles and (**c**) 6 cycles.

3.3.3. Analysis of Pore Structure of the CS-CG Stabilized Soil under Different Freeze-Thaw Cycles

(1) Porosity

As shown in Figure 12, the variation of porosity under different freeze-thaw cycles at different ages can be seen that:

a.　At the age of 7 d, with the increase of freeze-thaw cycles, the porosity increased slowly, and the porosity had increased by 0.4% after 6 freeze-thaw cycles. It displayed that the freeze-thaw cycles had little effect on it, which was related to the continuous hydration of the stabilized soil during freeze-thaw cycles.

b.　At the age of 28 d, with an increase in freeze-thaw cycles, the porosity increased first, then decreased and then increased, which was contrary to the UCS rule. The porosity had a direct impact on the UCS, and the largest influence on the formation of its porosity came during the first freeze-thaw cycle. After 6 freeze-thaw cycles, the porosity had increased by 2.1%.

c.　Comparing the porosity of two ages, it was evident that the porosity of 7 d was larger than 28 d, but the porosity increase after the freeze-thaw cycle was much smaller than 28 d. This is because the hydration of the 7 d sample was incomplete, the hydration reaction was more intense during the thawing process, and the formation of hydration products filled pores to a certain extent.

(2) Pore diameter

The effects of freeze-thaw cycles on pore diameter are shown in Figure 13.

As Figure 13 shows that,

The pore diameter distribution of the two ages was basically the same. As the freeze-thaw cycles increased, the percentage of pores with a diameter d < 100 nm decreased, and with diameter d > 1000 nm increased. It was mostly distributed in the 100~1000 nm range. Combined with previous studies on pores, it can be seen that the pore diameter was 10~100 nm and <10 nm, respectively, for transition pores and gel pores. Transition pores are pores between hydration products, as ettringite, $Ca(OH)_2$ crystals and C-S-H gel. Gel pores are interconnected pores between gel particles [32]. Therefore, As the freeze-thaw cycles increased, under the condition that the total amount of hydration products remains

unchanged, the small pores between hydration products and gel particles were transformed into large pores, which reduced the UCS of the CS-CG stabilized soil to a certain extent.
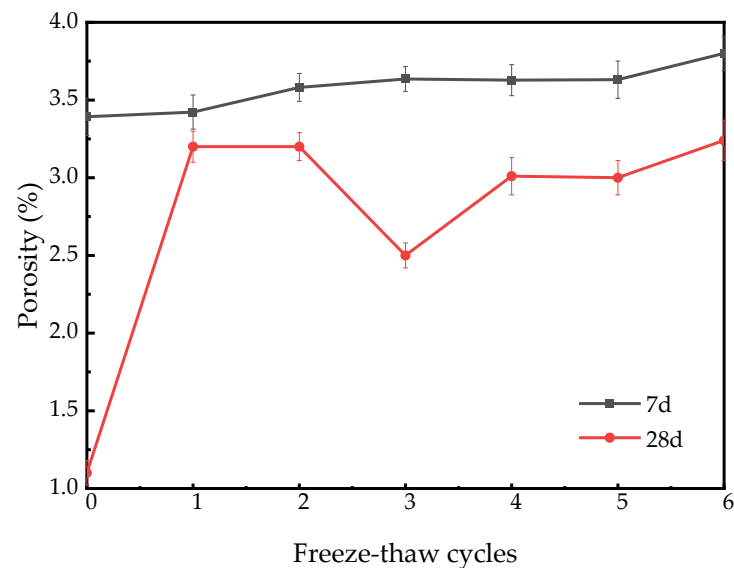

Figure 12. Porosity variation under different freeze-thaw cycles at different ages.
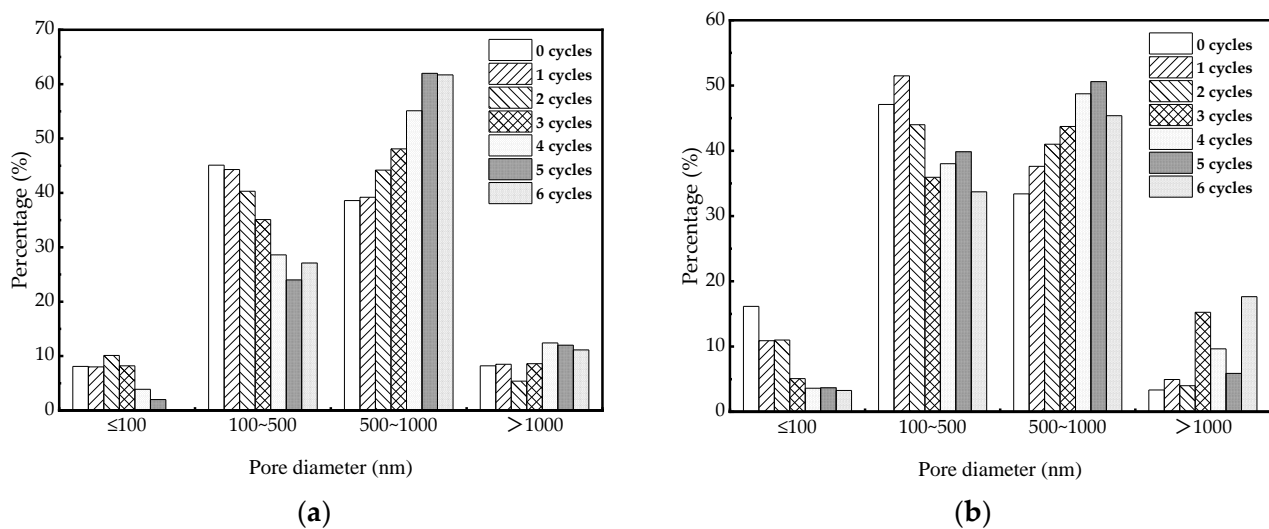

(**a**)   (**b**)

Figure 13. Effects of freeze-thaw cycles on pore diameter. (**a**) 7 d and (**b**) 28 d.

(3) Pore abundance

The effects of freeze-thaw cycles on pore abundance are shown in Figure 14. It can be seen from Figure 14 that,

a.   At the age of 7 d, the pore abundance increased obviously in the range of 0~0.2 and 0.2~0.4 after freeze-thaw cycles. The pores in the range of 0.6~0.8 were reduced. It was evident that the freeze-thaw cycles made the pores tend to be irregular. In addition, the freeze-thaw cycles led to the increase of cracks and greatly reduced the pore abundance.

b.   At the age of 28 d, freeze-thaw cycles increased the abundance in the range of 0.4~0.6. The decrease of pores in the range from 0.6 to 0.8 also caused the decrease of pore abundance, and there were no large cracks compared with the 7 d. The frost resistance of 28 d was better than 7 d.
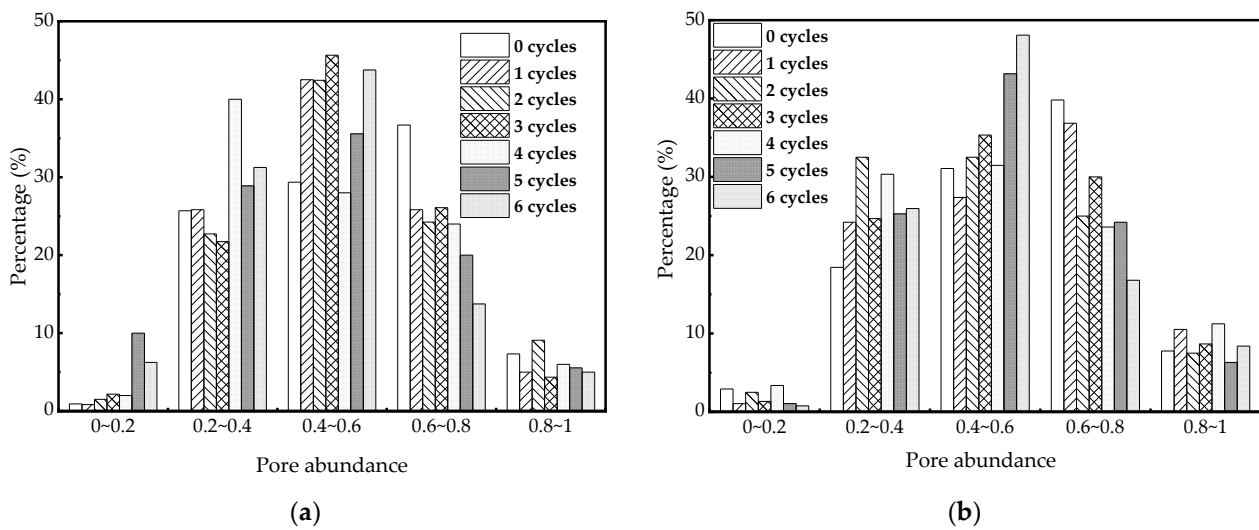
Figure 14. Variation of pore abundance under freeze-thaw cycles. (**a**) 7 d and (**b**) 28 d.

In summary, the freeze-thaw cycle will increase the pores and cracks, which will lead to the decrease of strength. However, with the increase of age, the hydration products in the stabilized soil increase, which reduces the trend of pore increase, and the performance is more superior.

4. The Freeze-Thaw Cycle Degradation Model of CS-CG Stabilized Soil

4.1. The Freeze-Thaw Cycle Degradation Model of CS-CG Stabilized Soil Based on Porosity Variation

According to the relevant literature, the rock freeze-thaw deterioration model was improved [3,33,34]. Based on the porosity variation of the CS-CG stabilized soil, a freeze-thaw cycle deterioration model of CS-CG stabilized soil was proposed, and the hypothesis derivation and verification of the model were carried out.

4.1.1. Model Assumptions

Assumption 1: The CS-CG stabilized soil has a continuous and uniform structure.

Assumption 2: The SLR of the CS-CG stabilized soil is proportional to the cycles of freeze-thaw, that is, the SLR per unit cycles of freeze-thaw is a constant.

Assumption 3: The porosity variation of the CS-CG stabilized soil is proportional to the cycles of freeze-thaw, that is, the porosity variation per unit number of freeze-thaw cycles is a constant.

Assumption 4: The porosity variation of the CS-CG stabilized soil is favorable correlated with the SLR, that is, the porosity variation and SLR have the same trend.

4.1.2. Model Derivation

According to the above model, it was assumed that the UCS of the CS-CG stabilized soil after n freeze-thaw cycles was $f(n)$, and $f(n)$ was differentiable. The UCS was f_0 when freeze-thaw cycles were 0. Therefore, SLR from n cycles to $(n + \Delta n)$ cycles is shown in Equation (3):

$$\frac{f(n) - f(n + \Delta n)}{f(n)} = \lambda_1 \Delta n \tag{3}$$

where λ_1 is SLR per unit number of cycles.

Equation (4) can be obtained from Equation (3).

$$\frac{f(n + \Delta n) - f(n)}{\Delta n} = -\lambda_1 f(n) \tag{4}$$

Equation (5) can be obtained from Equation (4).

$$\frac{df(n)}{dn} = -\lambda_1 f(n) \tag{5}$$

Equation (6) is obtained by integrating Equation (5).

$$f(n) = f_0 \exp(k_1 n) \tag{6}$$

After n freeze-thaw cycles, the porosity of CS-CG stabilized soil was $h(n)$, and $h(n)$ was differentiable. The porosity of the CS-CG stabilized soil was set to h_0 when the freeze-thaw cycles were 0, so the porosity variation from n freeze-thaw cycles to $(n + \Delta n)$ freeze-thaw cycles is shown in Equation (7):

$$h(n + \Delta n) - h(n) = \lambda_2 \Delta n \tag{7}$$

where is the porosity variation per unit number of cycles.

Equation (8) can be obtained from Equation (7).

$$\frac{h(n + \Delta n) - h(n)}{\Delta n} = \lambda_2 \tag{8}$$

Equation (9) can be obtained from Equation (8).

$$\frac{dh(n)}{dn} = \lambda_2 \tag{9}$$

Equation (6) is obtained by integrating Equation (5).

$$h(n) = h_0 + \lambda_2 n \tag{10}$$

Equation (11) can be obtained from Equation (10).

$$n = \frac{h(n) - h_0}{\lambda_2} \tag{11}$$

Substitute (11) into (6) to obtain (12).

$$f(n) = f_0 \exp\left\{-\frac{\lambda_1}{\lambda_2}[h(n) - h_0]\right\} \tag{12}$$

Equation (13) can be obtained from Equation (12).

$$\frac{f(n)}{f_0} = \exp\left\{-\frac{\lambda_1}{\lambda_2}[h(n) - h_0]\right\} \tag{13}$$

Let $h(n) - h_0 = \Delta h$ and $\lambda = \frac{\lambda_1}{\lambda_2} (\lambda > 0)$ was degradation factor of CS-CG stabilized soil UCS under freeze- thaw cycles. Taking into account the influence of different ages on the UCS of CS-CG stabilized soil, the correction factor β was introduced to correct it.

4.2. Validation of the Freeze-Thaw Cycle Degradation Model of CS-CG Stabilized Soil

Based on the model, the Y = β × exp(−λX) model was used to fit the UCS residual rate and porosity variation of the CS-CG stabilized soil under freeze-thaw cycles. The fitting results of freeze-thaw cycles degradation model are displayed in Figure 15. The statistical modeling result is shown in Table 3, where the UCS residual rate is expressed as F, the porosity variation is expressed as P, and the subscript is the age. For example, the UCS residual rate of 7 d age is expressed as F_7. The model fitting parameters are displayed in Table 4. It demonstrated that R^2 was greater than 0.98 at both ages, indicating that the UCS residual ratio at different ages had a good correlation with the porosity variation. The

degradation model was independent of the age and the cycles of freeze-thaw, so the UCS after freeze-thaw cycles could be evaluated by the porosity variation.
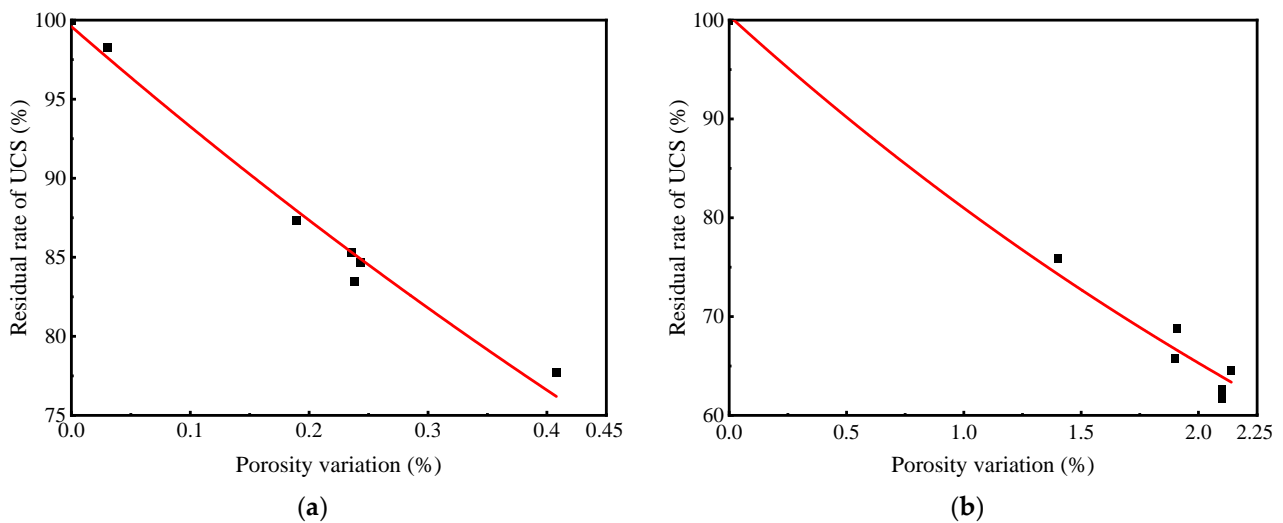

Figure 15. Fitting results of the freeze-thaw cycle degradation model. (**a**) 7 d and (**b**) 28 d.

Table 3. Statistical modeling result.

P_7 (%)	F_7 (%)	R^2	P_{28} (%)	F_{28} (%)	R^2
100.00	0.00		100.00	0.00	
98.24	0.03		75.83	1.40	
87.33	0.19		62.59	2.10	
84.69	0.24	0.985	68.75	1.91	0.983
85.33	0.24		65.77	1.90	
83.49	0.24		61.72	2.10	
77.68	0.41		64.50	2.14	

Table 4. Model fitting parameters.

Parameters	λ	β
7 d	0.66	99.59
28 d	0.22	100.43

5. Conclusions

Through freeze-thaw cycle test, shrinkage test, microstructure analysis and the establishment of a freeze-thaw cycle degradation model, the primary conclusions are as follows:

(1) The CS-CG stabilized soil had good frost resistance, and the UCS at 7 d and 28 d was 2.86 MPa and 3.79 MPa, respectively, after 6 freeze-thaw cycles, which were 22.6% and 35.5% lower than those did not undergo freeze-thaw cycles. The SLR was far less than in the PC stabilized soil and lime stabilized soil.

(2) The dry shrinkage characteristics of the CS-CG stabilized soil were between those of the PC stabilized soil and lime stabilized soil, and it had good crack resistance. The temperature change had little effect on its shrinkage deformation. The temperature shrinkage coefficient at low temperature was 5.8×10^{-6}, which was much smaller than PC stabilized soil and lime stabilized soil.

(3) With the increase of the CS-CG dosage, the hydration products increased continuously. However, after the freeze-thaw cycles, large pores and cracks gradually appeared inside the stabilized soil, resulting in an increase of porosity and pore diameter and a decrease of pore abundance.

(4) By establishing the freeze-thaw cycles degradation model of CS-CG stabilized soil, it can be seen that there was a $f(n)/f_0 = \beta \exp(-\lambda \Delta h)$ relationship between the UCS residual rate and porosity variation of the CS-CG stabilized soil, which was independent of age and had a good correlation.

(5) The frost resistance and shrinkage performance of the CS-CG stabilized soil were better than those of the PC stabilized soil and lime stabilized soil, and it can also realize the resource utilization of industrial solid waste and promote sustainable development, and therefore can be used for subgrade soil improvement in regions with seasonal frozen soil.

(6) There are still some shortcomings in this study. In the future research, it should focus on the performance regulation of CS-CG stabilized soil, such as changing the type of soil, the fineness of carbide slag and coal gangue, and the type of alkali activator.

References

1. Zhan, Y.; Lu, Z.; Yao, H.; Xian, S. A Coupled Thermo-Hydromechanical Model of Soil Slope in Seasonally Frozen Regions under Freeze-Thaw Action. *Adv. Civ. Eng.* **2018**, *2018*, 7219826. [CrossRef]
2. Den, Q.S.; Chao, Z.; He, X.Z.; Chen, F.G.; Liu, X. Simulation of hydrothermal field difference and anti-frost heaving of highway subgrade with sunny-shady slopes in seasonally frozen regions. *J. Cent. South Univ. Sci. Technol.* **2022**, *53*, 3113–3128. [CrossRef]
3. Feng, G.; Xiong, X.; Zhou, K.P.; Li, J.L.; Shi, W.C. Strength deterioration model of saturated sandstone under freeze-thaw cycles. *Rock Soil Mech.* **2019**, *40*, 926–932. [CrossRef]
4. Li, G.S.; Zhao, Y.Q.; Zhang, W.D.; Xu, X.T. Influence of snow cover on temperature field of frozen ground. *Cold Reg. Sci. Technol.* **2021**, *192*, 9. [CrossRef]
5. Lu, Y.; Liu, S.; Zhang, Y.; Li, Z.; Xu, L. Freeze-thaw performance of a cement-treated expansive soil. *Cold Reg. Sci. Technol.* **2020**, *170*, 102926. [CrossRef]
6. Han, C.P.; Cheng, P.F. Micropore variation and particle fractal representation of lime-stabilised subgrade soil under freeze-thaw cycles. *Road Mater. Pavement Des.* **2015**, *16*, 19–30. [CrossRef]
7. Deng, J.; Zhao, J.J.; Zhao, X.; Yu, J.L.; Lei, C.; Lee, M.; Huang, R.Q. Effect of Glutinous Rice Slurry on the Unconfined Compressive Strength of Lime-Treated Seasonal Permafrost Subjected to Freeze-Thaw Cycles. *KSCE J. Civ. Eng.* **2022**, *26*, 1712–1722. [CrossRef]
8. Zhang, J.; Tan, H.; He, X.; Yang, W.; Deng, X. Utilization of carbide slag-granulated blast furnace slag system by wet grinding as low carbon cementitious materials. *Constr. Build. Mater.* **2020**, *249*, 118763. [CrossRef]
9. Sun, C.; Zhang, J.; Yan, C.; Yin, L.; Wang, X.; Liu, S. Hydration characteristics of low carbon cementitious materials with multiple solid wastes. *Constr. Build. Mater.* **2022**, *322*, 126366. [CrossRef]
10. Ren, C.; Wang, W.; Li, G. Preparation of high-performance cementitious materials from industrial solid waste. *Constr. Build. Mater.* **2017**, *152*, 39–47. [CrossRef]
11. Chen, Z.Q.; Zhu, Z.W.; Lyu, Y. Laboratory investigation on the strength and freezing-thawing resistance of fly ash based geopolymer stabilized soil. *Hydrogeol. Eng. Geol.* **2022**, *49*, 100–108.
12. Li, W.T.; Yi, Y.L. Use of carbide slag from acetylene industry for activation of ground granulated blast-furnace slag. *Constr. Build. Mater.* **2020**, *238*, 10. [CrossRef]
13. Cheng, J.; Zhou, J.; Liu, J.; Cao, X.; Cen, K. Physicochemical characterizations and desulfurization properties in coal combustion of three calcium and sodium industrial wastes. *Energy Fuels* **2009**, *23*, 2506–2516. [CrossRef]
14. Cong, P.; Mei, L. Using silica fume for improvement of fly ash/slag based geopolymer activated with calcium carbide residue and gypsum. *Constr. Build. Mater.* **2021**, *275*, 122171. [CrossRef]
15. Guo, W.; Zhang, Z.; Zhao, Q.; Song, R.; Liu, J. Mechanical properties and microstructure of binding material using slag-fly ash synergistically activated by wet-basis soda residue-carbide slag. *Constr. Build. Mater.* **2021**, *269*, 121301. [CrossRef]

16. Lang, L.; Chen, B.; Li, N. Utilization of lime/carbide slag-activated ground granulated blast-furnace slag for dredged sludge stabilization. *Mar. Georesources Geotechnol.* **2020**, *39*, 659–669. [CrossRef]

17. Du, Y.J.; Liu, S.Y.; Wei, M.L.; Zhu, J.J. Micromechanism of over-wet clayey soils stabilized by calcium carbide residues. *Chin. J. Rock Mech. Eng.* **2014**, *33*, 1278–1285. [CrossRef]

18. Du, Y.J.; Liu, S.Y.; Qin, X.G.; Wei, M.L.; Wu, J.F. Field Investigations on Performance of Calcium Carbide Residues Stabilized Over-wet Clayey Soils Used as Highway Subgrade Materials. *J. Southeast Univ. Nat. Sci. Ed.* **2014**, *44*, 375–380. [CrossRef]

19. Li, P.L.; Pei, Y.; Hu, J.C.; Hu, W. Research on Influencing Factors and Prediction Model of Compressive Strength of Carbide Slag Stabilized Soil. *Mater. Rep.* **2021**, *35*, 22092–22097. [CrossRef]

20. Zhu, Y.; Zhu, Y.; Wang, A.; Sun, D.; Liu, K.; Liu, P.; Chu, Y. Valorization of calcined coal gangue as coarse aggregate in concrete. *Cem. Concr. Compos.* **2021**, *121*, 15. [CrossRef]

21. Huang, G.; Ji, Y.; Li, J.; Hou, Z.; Dong, Z. Improving strength of calcinated coal gangue geopolymer mortars via increasing calcium content. *Constr. Build. Mater.* **2018**, *166*, 760–768. [CrossRef]

22. Wang, S.; Luo, K.; Wang, X.; Sun, Y. Estimate of sulfur, arsenic, mercury, fluorine emissions due to spontaneous combustion of coal gangue: An important part of Chinese emission inventories. *Environ. Pollut.* **2016**, *209*, 107–113. [CrossRef] [PubMed]

23. Long, G.; Li, L.; Li, W.; Ma, K.; Dong, W.; Bai, C.; Zhou, J.L. Enhanced mechanical properties and durability of coal gangue reinforced cement-soil mixture for foundation treatments. *J. Clean. Prod.* **2019**, *231*, 468–482. [CrossRef]

24. Zhang, Y.; Wang, M.L.; Yin, X.X.; Feng, X.B. Effect of wetting-drying cycle on behavior of coal gangue-stabilized expansive soil. *Bull. Chin. Ceram. Soc.* **2018**, *37*, 3604–3610. [CrossRef]

25. Wang, J.; Wang, Q.; Lin, S.; Han, Y.; Cheng, S.; Wang, N. Relationship between the Shear Strength and Microscopic Pore Parameters of Saline Soil with Different Freeze-Thaw Cycles and Salinities. *Symmetry* **2020**, *12*, 19. [CrossRef]

26. Xu, S.M.; Wu, Z.J.; Zhao, W.C.; Zhao, T. Study of the Microscopic Pores of Structured Loess Based on Matlab and IPP. *China Earthq. Eng. J.* **2017**, *39*, 80–87. [CrossRef]

27. Miao, D.Y. *Study on Processing Method of Sem Soil Image Based on MATLAB*; Taiyuan University of Technology: Taiyuan, China, 2014.

28. *JTG 3430-2020*; Test Methods of Soils for Highway Engineering. China Communications Press Co., Ltd.: Beijing, China, 2020.

29. Xu, B.; Liu, Q.; Ai, B.; Ding, S.; Frost, R.L. Thermal decomposition of selected coal gangue. *J. Therm. Anal. Calorim.* **2017**, *131*, 1413–1422. [CrossRef]

30. *JTG E51-2009*; Test Methods of Materials Stabilized with Inorganic Binders for Highway Engineering. China Communications Press: Beijing, China, 2009.

31. Sun, Q.; Gong, X.L.; Zhang, Y.L.; Xu, T.Y. A study of the dynamic experimental of clay desiccation cracking process. *Hydrogeol. Eng. Geol.* **2014**, *41*, 144–147.

32. Powers, T.C. Structure and Physical Properties of Hardened Portland Cement Paste. *J. Am. Ceram. Soc.* **1958**, *41*, 1–6. [CrossRef]

33. Liu, T.Y.; Zhang, C.Y.; Cao, P.; Zhou, K.P. Freeze-thaw damage evolution of fractured rock mass using nuclear magnetic resonance technology. *Cold Reg. Sci. Tech.* **2020**, *170*, 13. [CrossRef]

34. Liu, T.; Cui, M.; Zhang, C.; Zhou, K.; Shi, W.; Cao, P. Nuclear magnetic resonance analysis of the failure and damage model of rock masses during freeze-thaw cycles. *Bull. Eng. Geol. Environ.* **2022**, *81*, 21. [CrossRef]